

1 Introduction

1.1 Nanotube Overview

In 1991, Iijima discovered carbon nanotubes (CNTs) accidentally while studying manufacturing methods for fullerenes[1]. Instead of atomic carbon spheres, he found elongated tubes with diameters in the nanometer range and lengths in the micron range. The tubes were found to be closed cylindrical structures with a hexagonal bonding similar to that in graphite. The similarity in atomic structure between nanotubes and fullerenes is shown in Figure 1.1. In this example the tube is closed at its ends by endcaps that are hemispheres of fullerenes. In general, the smooth interface shown is not possible because a hemispherical geometry is often precluded by other nanotubes structures, but all nanotubes are naturally closed by endcaps of some sort.

The scientific and engineering community has embraced the discovery of nanotubes due to their excellent properties and wide ranging potential. Jamieson[2] argues that nanotechnology, mainly due to CNTs, may impact technology more than the silicon revolution. CNTs can have electrical properties that range from metallic to semiconductor in nature depending on their atomic structure. The mechanical properties of CNTs provide great potential for a variety of applications. They possess exceptionally high specific stiffness and strength, with values estimated in the range of 1 TPa for modulus and 10-12% strain to failure[3, 4]. Carbon nanotubes have also been found to be extremely elastic, being able to reverse bend through 360 degrees without accumulating damage[5]. These excellent mechanical properties are primarily due to their hybridized bonds and tightly closed atomic structure.

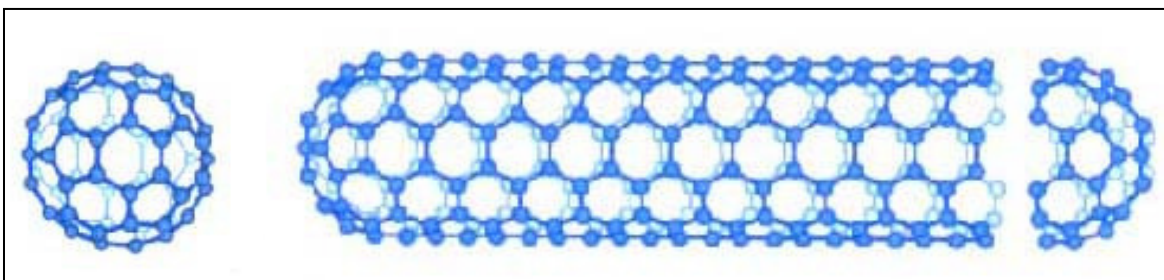


Figure 1.1. Atomic structures of a C₆₀ fullerene (left) and a (5,5) nanotube (right)

The tube shown in Figure 1.1 is an example of a single wall nanotube (SWNT). SWNTs are exactly one atom thick. The tubes found by Iijima were multiwalled nanotubes (MWNTs). MWNTs are essentially concentrically nested SWNTs. The individual tubes, or walls, are not bonded together. They only interact through the weak non-bonded van der Waals forces. The individual walls are ideally separated by 3.4 \AA , the same distance as the layer separation found in graphite sheets. They remain free to slide and rotate independently with only small resistive forces. Thus, it is expected that tension and torsion loads will not significantly transfer from outer tube walls to inner tube walls. However, the presence of endcaps can cause compressive load transfer through the van der Waals forces. Likewise, load transfer will occur between walls during both global and local bending. Thus, while the axial stiffness may not change with the addition of internal walls, the bending stiffness will definitely increase. A type of MWNT, a double walled nanotube (DWNT), is shown in Figure 1.2.

The primary structural unit of a nanotube is a hexagonal ring. The rings consist of sigma and pi bonds. Each atom is bonded to its nearest 3 neighbors, at approximately 120 degrees in plane angles. The primary bonds between these atoms are the hybridized sp^2 bonds, or sigma bonds. These bonds are very strong and produce the tubes excellent in-plane properties. The pi-bonds are delocalized bonds and are much weaker; however they are centered, symmetrically about 0.33 \AA from the central axis of the sigma bond. Thus they are primarily responsible for the out of plane properties, such as the wall bending stiffness. The hexagonal bond structure is shown in Figure 1.2. Pentagonal and heptagonal ring structures are also possible. A combination of these structures, termed the 5-7-7-5 defect, is proposed to be a pathway for plastic deformations and termed the Stone-Wales transformation[6-8]. Isolated changes in ring structure lead to temporary or permanent changes in tube radius. These ring structures are also found in fullerenes and endcaps. Quantum Mechanics (QM) simulations have also shown evidence of structural holes in nanotubes, which subsequently lower the nanotube stiffness and strength[9].

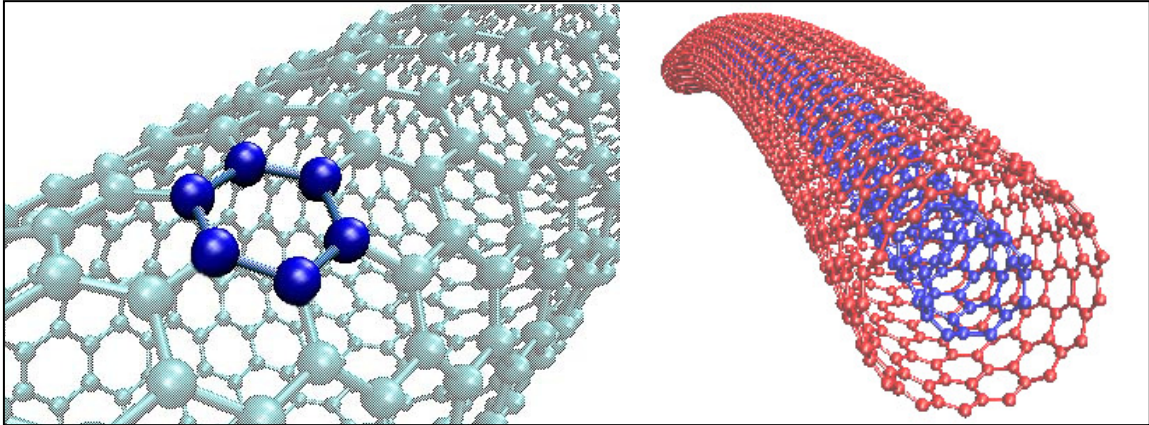


Figure 1.2. An SWNT with the hexagonal bond structure highlighted and a double wall nanotube

Numerous atomic structures are available to nanotubes, which are determined by the roll-up angle, termed helicity or chirality, and diameter of the hexagon ring structure. The White notation is commonly used to classify a nanotubes structure[10]. In this notation, the tubes are classified by the basal vector, which is followed to find the circumferential joining point of the hexagon structure. The number of hexagon rings required in the a and b vectors needed to travel once around the tube and close the structure atomically is written as (a,b) which also defines the helical angle, θ . Due to this structure only a discrete set of diameters are available to nanotubes.

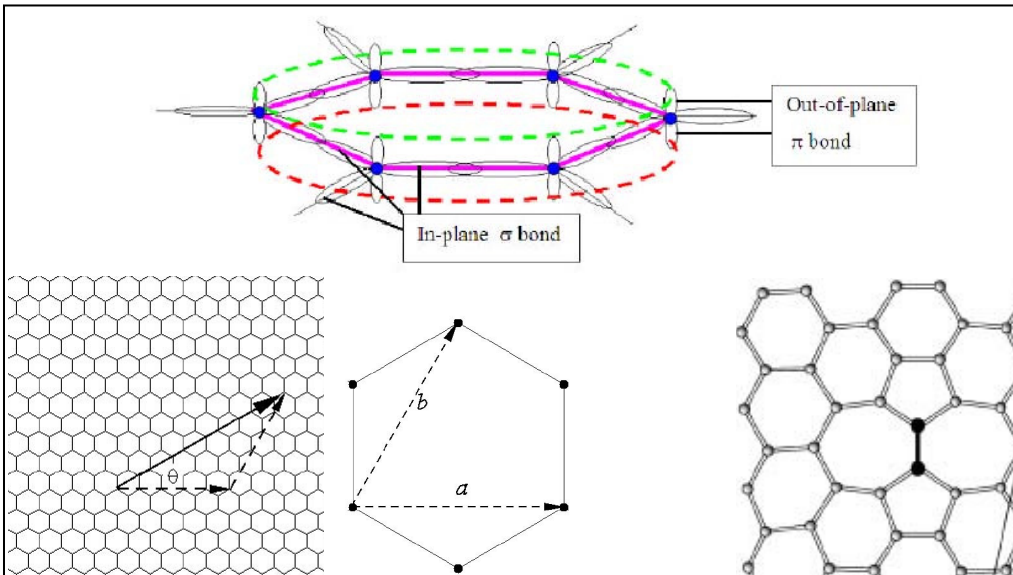


Figure 1.3. Schematics of the bonds and structure; (top), the sp^2 and π -bonds; (bottom, left), the roll-up vector; (bottom right), the 5775 Stone-Wales transformation

Nanotubes with different molecular structures, such as BN and BC₃ or ‘white carbon’ nanotubes (generalized as B_xC_yN_z), have also been created[11]. The fundamental feature required for nanotube creation is the hexagonal atomic ring structure. Numerous molecular combinations will form these hexagonal laminar sheets, some combinations are even inherently multiwalled. These tubes have been found to have lower mechanical properties, but also possess other desirable qualities for certain applications. For example, the ‘white carbon’ nanotubes, which still have ~68-75% the modulus of CNTs[11], are electrically inactive and therefore desirable for nanocomposites material applications which need an insulating material.

The potential applications for materials with these properties are immense. Their size and extraordinary properties make them candidates for replacing existing materials in applications as well as opening new technologies. For example, their stiffness, strength and aspect ratio give them the potential to be the ultimate fiber reinforcement for composite materials[12-15]. More subtly, their nanometer size would allow them to be injected into a mold, with the liquid resin, using the existing, standard infusion equipment and techniques for plastics. Some have even theorized that the fibers could subsequently be aligned using their electrical properties. However, great challenges must be first overcome to make nanotube composites feasible engineering materials. Currently nanotubes are almost prohibitively expensive which limits the size and volume fraction for even research samples. Nanotube adhesion may be questionable and needs to be examined in more detail. Manufacturing processing is presently difficult with dispersion problems prominent and high viscosity preventing flow.

Nanotubes could also be used to replace current micro-electronic materials (MEMs) as the beam structure, reducing MEMs sizes even further. MWNTs have been proposed as cylindrical bearings due to the ability of their walls to slide freely. Molecular modeling research has also been performed which studied the feasibility of using the tubes as the shafts for nanogears[16, 17]. CNTs have also been proposed as nanoscale drug dispensers[18].

To help realize their full potential, nanotube properties must be characterized by developing mathematical models. These models must subsequently be verified and quantified by performing and analyzing experiments. The following sections will detail

the two types of nanotube models, continuum and molecular, and two types of experiments, physical and virtual.

1.2 Nanotube Models

Nanotubes are a class of materials that falls into the burgeoning new field of multi-scale modeling. Multi-scale modeling is a method for modeling materials, systems or phenomena that differ on time or length scales of many orders of magnitude. Often, these large scale differences require different modeling techniques to capture various levels of phenomena which must be reconciled and incorporated. Nanotubes are single or nested molecules with dimensions on the angstrom level and important material responses occur at this discrete level. However, many of their potential uses, such as the response of nanotube-composite part, require macrolevel predictions and behaviors which encompasses 10 orders of magnitude size difference. Thus, methods must be employed which can bridge the gaps between models and size scales. A new research paradigm for research into nanostructured materials is emerging which uses multi-scale modeling and the new powerful computing resources now available which is termed “Computational Materials”[19].

The various modeling techniques/methods for nanotubes, loosely from the smallest to largest scale, are molecular (atomistic) simulations, coarse grain simulations, continuum mechanics, composite micro-mechanics, and component level structural mechanics. This study will focus on nanotubes, and not their applications, and thus will only investigate models appropriate to nanotubes, molecular simulations and continuum mechanics. The continuum models are generally based on traditional engineering models such as beams, shells or membranes. They treat nanotubes as continuous materials with definite geometries and common material properties such as Young’s modulus. In contrast the molecular models consider each atom and mathematically define the interactions between the atoms. Often, the molecular models are reduced to continuum models so that the results can be compared with other continuum models and other materials directly. The subsequent sub-sections cover the basic theory behind the models. Results using specific nanotube models are detailed and compared in Sections 1.3 and 1.4, Experimental Testing and Molecular Simulations, respectively.

1.2.1 Continuum Models

Based on his work with atomistic simulations of nanotubes, Yakobson stated one of the early results on nanomechanics, “the laws of continuum mechanics are amazingly robust and allow one to treat even intrinsically discrete objects only a few atoms in diameter[20].” This allowed subsequent researchers to utilize continuum mechanics to classify CNT material properties with more assurity. Numerous choices for the continuum model are possible and include the aforementioned beam, shell and membrane models. The choices facing the analyst are effectively reduced to those of geometry, assumptions on deformations, and constitutive laws.

The choice of geometry is less clear than may be at first apparent. The nanotube model may be a solid, hollow cylinder or nested cylinders (for MWNTs). A solid cylinder is often used to model nanotubes as fibers in composite materials. More commonly a hollow cylinder is chosen for each wall. The individual wall thickness is generally chosen to be the ideal wall separation distance for both graphite layers and nanotubes, 3.4 \AA . Generally, the walls are assumed to be perfectly bonded. This allows for a MWNT to be a single hollow cylinder, without gaps. The nanotube wall thickness is then, $t = 3.4 n \text{ \AA}$, where, t , is the total thickness and, n , the number of walls in the nanotube. Typically, this cylinder geometry is coupled with the assumption of isotropy, which creates the standard model found in the literature. This is the material model that yields the often quoted $\sim 1 \text{ TPa}$ value for Young’s modulus. This thickness also corresponds to the mass density of a nanotube with the mass density of graphite. Generally this material model is analyzed as a beam or column model. Note that the assumption of a perfect bond means that each wall of a MWNT can be axially or torsionally engaged when the outer wall is subjected to such a load. This may become a source of error since the individual walls of MWNTs have been shown to be in or near a free slip condition[3].

The choices for the standard model were based on molecular physics phenomena and ease of use. However, closer examination reveals that the choices may be flawed. For instance, a carbon nanotube wall is one atom thick. What is the thickness of an atom? Nanotube wall thickness is certainly an abstract idea. Similarly, stress in a nanotube is also an abstract idea. Through-thickness stress in a single wall is assumed to be zero.

Naturally the choice of wall thickness will affect the continuum stress state. Arguments can be made for different values. The validity of the choice is really determined by the ability of the overall model to properly predict mechanical responses.

Another common model, proposed by Yakobson et al., uses the pi-bond thickness to define the thickness of an atom and thus the wall thickness[20]. This thickness is 0.66 Å, which leaves a gap between walls of a MWNT, and necessitates a nested, concentric cylinder model. A schematic of the concentric cylinder model is shown in Figure 1.4. They argue that this thickness is better able to describe the local bending stiffness of the nanotube. They compare axial shell wall buckling predictions to molecular mechanics simulations to support this hypothesis. With this reduced thickness, Young's modulus rises to ~5.5 TPa to keep the nanotube stiffness the same for the two models. However, it should be noted that the choice of thickness was predicated on a molecular physics model and not continuum mechanics assumptions or relationships.

The most common material response assumptions are that nanotubes are isotropic and linear elastic materials. Neither assumption can be studied experimentally due to the scale and poor resolution. It might be expected that some directional dependence may be induced by either the hexagonal ring structure or the residual strain induced by rolling the lamellar graphitic structure. Currently, these assumptions may only be studied through molecular simulations. The argument for transverse isotropy is easily generated from the nanotube geometry. The assumption that mechanical response of the tube is independent of chirality dictates that the stiffness of the wall is independent of direction. In contrast the radial direction of the tube is obviously different than the cylindrical surface because it does not share the graphitic bonding structure. The concept of through-thickness strain (radial strain) and stress is non-existent for SWNTs. However, for MWNTs the wall separation distance may change, which would be radial strain. Here, the resistance to strain is provided only by van der Waals forces, thus the stiffness would necessarily be different.

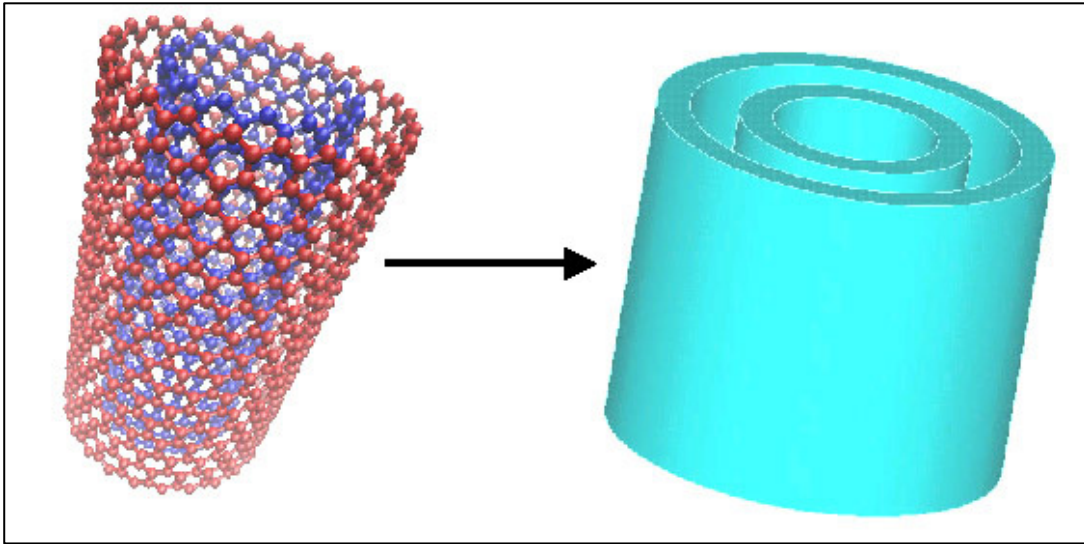


Figure 1.4. A continuum structure equivalent (right) compared to a molecular model

The assumptions about the nanotube deformation suggest the type of continuum model. For example, the assumption that plane cross sections remain plane in bending constitutes a Euler-Bernoulli beam model. Beam and shell models are the most common in the literature. However, other models have been studied and some will subsequently be summarized. Some just adapt beam or shell models directly, while others are more elaborate. Most of these finite element (FE) models have been developed for more complex models incorporating independent MWNT wall movement or composite materials.

For MWNTs, once a model has been defined for the tube walls, a model for wall interaction must also be developed. For beams, this model is simply uniform motion, which means a perfectly rigid connection. Other models allow for independent wall movement of some sort where the interaction is a function of the local wall separation distance. The most direct equivalent to the van der Waals forces is pressure. Ru used such an approach to study the effect of van der Waals forces on the buckling response of a DWNT[21]. He modeled the tube walls as shells with a bending stiffness, $D(h) = Eh^3/(12(1-\nu^2))$, where h is the wall thickness and ν Poisson's ratio. He assumed that the shell walls interact through pressure, p , given by, $p_i R_i = p_j R_j$, where R is the wall radius and superscripts i and j signify wall numbers. His analysis predicts that the critical strain

for buckling of a SWNT is lowered by the addition of an inner wall. He found neither the buckled shapes nor the pressure due to van der Waals forces.

One important advantage of FE models is their ability to model interwall interactions with discrete methods, such as truss elements. Pantano et al. used such an approach to model a MWNT[22, 23]. The walls were modeled as thin shells while the inter-wall interactions were modeled as pressures. The pressures were defined as functions of separation distance. They implemented this function into the FE model using a user subroutine interactive element in ABAQUS/Standard. They then validated this model for SWNTs and MWNTs by comparing the FE results versus molecular mechanics simulations and experimental results in bending and pressure loads. They found good predictions for strain energies, local buckling strain initiations and kinking modes for SWNTs in bending. In nanotube reinforced composites, a nanotube may be forced into a highly curved deformed shape by the polymer which causes a buckling mode termed rippling. This mode shape can be seen experimentally in transmission electron microscope (TEM) images[24]. The number and wavelengths of the ripples is a function of the load (curve), and number of walls. It is an important phenomenon for observing the wall interaction. Using TEM images, Pantano et al. were able to predict reasonable rippling behavior for a nanotube with the same number of walls (and diameters) at similar bending curvatures.

Arroyo and Belytschko also developed a FE model for MWNTs[25]. Rather than using a thin shell theory, they developed a membrane wall model directly from the Tersoff-Brenner potential using generalized crystal elasticity and a modified Cauchy-Born rule. The resulting model is hyperelastic and depends on the surface curvature and the crystal lattice orientation. They model the van der Waals forces by placing the Lennard-Jones equation into the weak formulation of their FE code. They were able to reproduce local buckling, kinking and rippling effects, which are nearly identical to the deformed states of the parent molecular simulation, by using fine meshes for a variety of loadings including compression, torsion and bending.

Others have taken a much different FE approach, whereby typical molecular mechanics (MM) variables are replaced by truss elements. In such approaches, the bond length is represented by a truss element with a stiffness derived from the MM bond

stretching potential. Other energy terms such as bond angle and van der Waals forces are likewise replaced with trusses of various stiffnesses. These methods essentially linearize MM equations and place it into a FE framework. Based on potentials for bond deformations and van der Waals forces, Li and Chou created a truss model for a DWNT[26]. When only the outer wall was loaded, they found little to no transfer of load to the inner wall. Their work shares much in common with MM, and reports results in terms of the standard continuum model.

1.2.2 Molecular Models

Due to the current limitations with nanoscale mechanical tests, molecular simulations serve as important tools for studying nanotube mechanics. They can be used in two manners; to replace experimental testing, providing data for continuum models, or to directly predict mechanical responses for specified load conditions. Molecular simulations offer several advantages over experimental testing. First, they are much less expensive to perform. Second, they have a wider range of testing potential. Tests that are currently not experimentally feasible, such as torsion tests, are easily performed, only requiring the proper application of boundary conditions. Third, they are much more precise than experiments. Current experiments are plagued by poor resolution, which can be mitigated in molecular simulations. However, it must be noted that molecular simulations are only estimations. They are based on numerous assumptions and simplifications. All conclusions drawn from molecular simulations should be tempered with this knowledge. This means that molecular models should be used as tools to understanding nanotubes and physical experimental data preferred when available.

Two main types of molecular simulations are available to the analyst, molecular mechanics (MM) and quantum mechanics (QM). The major difference between the two is that MM models are derived empirically and QM models are developed from first principles. In general QM results are deemed more accurate than MM. However, QM models are massively more computationally expensive than MM. Thus, QM models are usually confined to smaller systems, less than 100 atoms, which can severely limit nanotube QM studies.

1.2.2a Quantum Mechanics.

As previously mentioned, QM models are based on first principle approaches. The starting point for QM is the Schrodinger wave equation. It is a second order eigenvalue equation that cannot be solved exactly for any molecular system. To simplify the problem, the Born-Oppenheimer approximation is applied. It states that the electron masses, and therefore momenta, are orders of magnitude lower than those of the heavy nucleus. This allows for the uncoupling of nuclei and electron equations. The electrons are thus able to react instantaneously to changes in nuclei positions. Some of the more common methods for quantum mechanical solutions are molecular orbitals, ab-initio, semi-empirical and density functional theory. Without digressing into a discussion outside the scope of this study, several points can be made about each. Molecular orbital approaches are generally not used for complex systems, but have been used to study pi-bond systems for aromatic carbon rings[27]. Ab-initio methods are the most rigorous methods and are most truly based on first principles. Semi-empirical methods simplify some integrals or terms in the Schrodinger equation, but have been argued to be just as accurate as ab-initio methods which rely on calibration. Density functional theory (DFT) is a popular method for material scientists. DFT does not calculate the full wavefunction but instead calculates the electron density. For a detailed view of QM the reader is referred to a molecular simulations text by Leach[28]. Some QM results for nanotube property predictions are given in Section 1.3 alongside MM results.

A major advantage of QM is the ability to model chemical changes, especially bond breaking. Troya concludes that MM do not properly predict nanotube failure[9]. He studies the Stone-Wales defect and bond fracture using two semiempirical models and two MM models (see next section). He shows that the MM models incorrectly predict the bonds that open under axial strain, in the Stone-Wales defect, as compared to the more theoretically rigorous QM models. He also concludes that this particular MM potential gives an abnormally low nanotube modulus (~0.82 TPa). Other QM studies, which have focused more on modulus prediction, are presented as results in the molecular simulations section (1.4).

1.2.2b Molecular Mechanics.

MM is a method for modeling the atomic bonding and forces present in and between molecules. It has been used to study a wide range of problems from DNA dynamics to crack propagation in metals. It utilizes the Born-Openheimer approximation to reduce the atomic interactions to those between the nuclei. Each atom interacts with its bonded and non-bonded neighbors through a potential energy function. In its most common form, the pair-wise potential, each interaction is represented by a separate term. Usually these terms are polynomial or trigonometric functions; however, exponential forms have also been used. These more complex interactions are typically used for specific classes of problems. Two potentials are used in the present study, the MM3 and Tersoff-Brenner (TB) potential. The MM3 potential is a general hydrocarbon potential, while the TB potential is specific to diamond and graphitic structures. The most common variables in pair-wise potentials are shown in Figure 1.5. For a more complete discussion of MM the reader is referred again to the text by Leach[28].

The MM3 potential is a class II pair-wise potential with both higher-order expansions and cross-terms[29]. While this potential is a general potential, including hundreds of types of atoms, it is considered an accurate potential due to its higher order nature. For example, the quartic expansion of the bond stretching term serves to expand the range of accuracy to higher values of bond strains (see Figure 1.6). The potential requires *apriori* bond connectivity information and cannot model bond breaking or strength. It is used primarily to study biochemistry problems involving DNA and proteins. It is an appropriate model to study CNTs due to the similarity between sp^2 bonds in the hexagonal graphitic structure of nanotubes and the hexagonal structure of aromatic proteins.

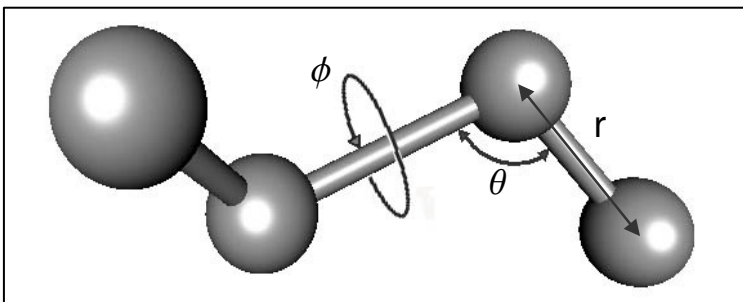


Figure 1.5. Common molecular mechanics variables

The MM3 potential is shown below in equation set (1.1) [29]. The set includes primary terms for bond stretching (U_s), bond angle bending (U_θ), and bond torsion (U_ϕ). The cross terms are stretch-bend ($U_{s\theta}$), angle-angle ($U_{\theta\theta}$), and out-of-plane bend ($U_{\phi s}$). The van der Waals force term (U_{vdw}), follows an exponential term and r^{-6} term. The independent variables in Figure 1.4 are r , θ and ϕ . A subscript, 0, on a variable signifies its value in the unstressed, equilibrium configuration. The total energy of a body equals the sum of the potential for all atoms in the body (in eqn. (1.1) , the indices i and k range over all atoms and the index j ranges over bonded atoms). Values of constants $r_0, \theta_0, K_s, K_\theta, V_1, V_2, V_3, \epsilon, \gamma, K_{sb}, K_{\phi s}$ and $K'_{\theta\theta}$ are given by Ponder[30].

$$\begin{aligned}
U_s &= 71.94K_s(r - r_0)^2[1 - 2.55(r - r_0) + (\frac{7}{12})2.55(r - r_0)^2] \\
U_\theta &= 0.02191K_\theta(\theta - \theta_0)^2 \times \\
&\quad [1 - (\theta - \theta_0) + 5.6(10^{-5})(\theta - \theta_0)^2 - 7.0(10^{-7})(\theta - \theta_0)^3 + 9.0(10^{-10})(\theta - \theta_0)^4] \\
U_\phi &= (V_1 / 2)(1 + \cos \phi) + (V_2 / 2)(1 - \cos 2\phi) + (V_3 / 2)(1 + \cos 3\phi) \\
U_{vdw} &= \epsilon\{-2.25(r_v / r)^6 + 1.84(10^5) \exp[-12.00(r / r_v)]\} \\
U_{sb} &= 2.511K_{sb}[(r - r_0) + (r' - r'_0)](\theta - \theta_0) \\
U_{s\phi} &= 11.995(K_{\phi s} / 2)(r - r_0)(1 + \cos 3\phi) \\
U_{\theta\theta'} &= -0.021914K_{\theta\theta'}(\theta - \theta_0)(\theta' - \theta'_0)
\end{aligned} \tag{1.1}$$

Note that the out-of-plane bending term may potentially be important in two ways. First, it is included to help keep the hexagonal bond structure planar, which is forced into curvature by the closed nature of nanotubes. This may differentiate nanotube responses from that of planar graphite. Second, this term will influence the bending stiffness of the nanotube by introducing a resistance to out of plane movements. This may play out in both the global bending and shell wall buckling responses.

This potential was chosen for its accuracy, ease of use and generality, which includes the ability to study many different types of polymers because of its numerous atom types. The Tinker molecular modeling package was used to model the nanotubes with the MM3 potential with MM[30]. Tinker is a freeware modeling program developed by Dr. Ponder and associates at Washington University in St. Louis. The program incorporates several different MM potentials by altering their forms to fit the Tinker potential form (these

altered potentials were verified for numerous cases versus the original before distribution).

The TB potential is an empirical bond-order potential specifically designed for diamond and graphite structures[31, 32]. The bond strength is a pair-wise potential function of the atomic separation, angle and the number of bonds (neighbors). The basic form of the TB potential sums the energies between atoms i and j , and is given in equation (1.2), where r is the distance between atoms, V_R and V_A are the repulsive and attractive terms respectively, and B_{ij} is the bond order.

$$U = \sum_i \sum_{j(>i)} V_R(r_{ij}) - \overline{B_{ij}} V_A(r_{ij}) \quad (1.2)$$

Rather than using a polynomial function to define the bond strength, the first generation TB potential[31] uses exponential functions similar to the Morse[28] potential. The second generation TB potential[32] modifies the attractive and repulsive exponential terms to more properly fit equilibrium distances, energies and force constants. The number of neighbors within a prescribed distance determines the number of bonds for an atom (B_{ij}). The number of bonds, or bond order, helps define the bond strength of the pair-wise bond potential. Thus bond breaking or redistribution (such as the Stone-Wales 7-5-5-7 defect) can also be studied using this potential. The program used to implement this potential (brennermd) for the present study was authored and distributed by Dr. Brenner at North Carolina State.

The bond stretching terms of the two potentials described above are compared to the Amber[33] and Morse[28, 34] potentials in Figure 1.6, for sp² bonds. The Amber potential is a simple pair-wise potential used for large molecular structures. Its bond stretching term is quadratic and thus symmetric about its equilibrium distance. This term yields a linear spring relationship between the bonded atoms. It is useful as a reference point in this comparison. The Morse potential is an exponential function, which is thought to give a very accurate bond strain relationship. In this comparison, it is viewed as the most accurate response. First, notice that the parabolic relationship differs greatly from the other three responses. The range of its accuracy is limited to strains very close to equilibrium, perhaps $\pm 2\%$ strain. The other three responses are asymmetric about

equilibrium, with a stiffer response in compression than in tension. This implies that the spring constant of the bond stretching term is non-linear. Thus, the mechanical response of a nanotube will likely be nonlinear. The MM3 and TB potentials seem to be accurate up to $\pm 10\%$ axial strain.

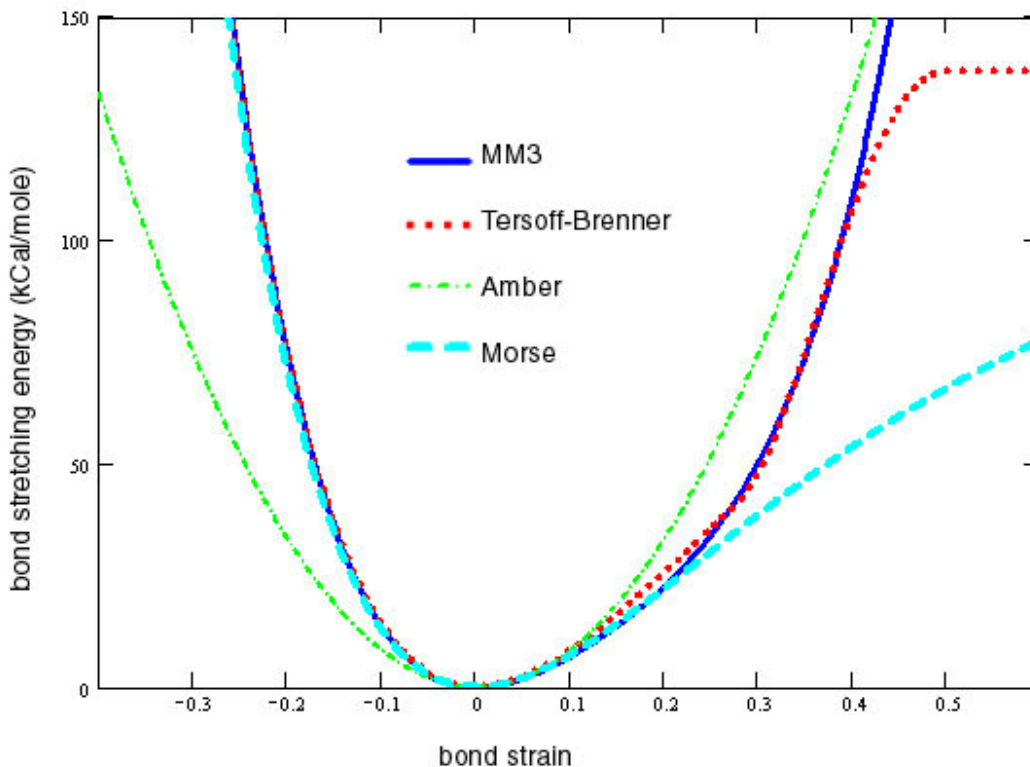


Figure 1.6. Comparison of bond stretching terms for four MM potentials

MM potentials quantify the energy level of a molecular system for a given structure. In the present study, the molecular structure is defined as the positions of the atoms of a molecule. In contrast, the system is defined as the whole state of the simulation, including all molecules, their positions, boundaries, and velocities (see MD below). Thus, strain energy is the difference between the potential energies of initial state and that of one deformed from that initial state. It is generally useful to find the minimum energy of a system, termed the relaxed structure. This relaxed structure is viewed as the unstressed state in engineering terms. Many techniques can be used to find this relaxed structure, which may be difficult to find for a given system. These techniques include well known algorithms such as steepest descent and Newton-Raphson, or less straight-forward techniques such as Monte-Carlo. In general, the potential energy of every initial,

user input structure must be minimized to alleviate contact or high strain problems. The straightforward minimization techniques often have difficulties finding global minimum for complex structures. Thus, it is often popular to use techniques such as Monte-Carlo or molecular dynamics which sample a greater energy surface.

Molecular dynamics (MD) is an extension of MM where the atoms are also imbued with momentum. Thus each atom has a given velocity as well as position, and the accelerations of the atoms are derived from the energy potentials. MD allows for a large range of structures to be analyzed as the system moves and vibrates. Temperatures may be prescribed for MD, which relate to the system's momenta. MD systems generally employ periodicity to keep the system compact, or to simulate a typical volume. Here, when an atom passes beyond the defined periodic box, it reappears on the opposite side of the box at a mirrored position. Various schemes are available to describe a system's dynamics, where the enthalpy, temperature, pressure or volume may be kept constant. In general, MD simulations will tend to 'converge' around a potential energy for the system, as compared to its initial state. The structure will continue to move and vibrate past local minima thereby potentially sampling a large range of structures. For a more complete description of minimization techniques and MD see Leach[28].

1.3 Experimental Results

The mechanical experiments on nanotubes have been generally performed on either individual nanotubes or nano-composite materials. The experiments on individual tubes have focused on recreating simple material properties tests on the nanoscale. Many traditional, and simple mechanical tests at the macro-level become extremely difficult to perform or measure at the nanoscale. For example, the question of gripping a single nanotube is nontrivial. Despite these difficulties many tests have successfully performed on both single and multiwalled tubes. The most common tend to be bending tests, particularly cantilever[35] and 3-point bending[36, 37]. However, successful tension tests have been performed[3, 38], and one of the first tests to be performed was a vibrations test[39]. Numerous tests and results are listed in Table 1.A. For a more comprehensive review of nanotube experimentation, the reader is referred to the review by Qian et al[40].

Table 1.1. Material property results from CNT mechanical experiments

investigation	year	Young's modulus (TPa)	deviation (TPa)	test	tube
Treacy et al.[39]	'96	1.8	1.4	thermal vibrations	mwnt
Wong et al.[35]	'97	1.28	0.6	cantilever	mwnt
Krishnan et al.[41]	'98	1.3	0.5	thermal vibrations	swnt
Salvetat et al.[36]	'99	0.81	0.41	3 pt. bending	bundles
Salvetat et al.[36]	'99	1.28	0.59	3 pt. bending	mwnt
Tomblor et al.[37, 42]	'00	1.2	na	3 pt. bending	swnt
Cooper and Young	'00	0.78 - 2.34		raman spect.	swnt
Yu et al.[3]	'00	0.27 - 0.95		tension	mwnt
Lourie et al.[43]	'98	2.8 - 3.6		raman spectroscopy	swnt
Lourie et al.[43]	'98	1.7 - 2.4		raman spectroscopy	mwnt
Yu et al.[38]	'00	0.32 - 1.47		tension	ropes
Poncharal et al.[44]	'99	~1	na	electric vibrations	mwnt

Several trends can be noted in Table 1.A. First, the results are all in terms of the standard continuum model (linear, isotropic, $t = 3.4 \text{ \AA}$). This is understandable since it is the easiest to use and is the most common. Other models are typically only discussed with respect to molecular simulations. Second, the results tend to have very large scatter, which is understandable considering they are pushing the limits of nanoscale manipulation. It should also be noted that the quality of nanotubes used in the experiments also have an effect on the result and scatter of the data. The most commonly used instrument is atomic force microscope (AFM), which is used to apply loads to the nanotube in bending and tension tests. As stated earlier in this chapter, the commonly accepted value for Young's modulus is approximately 1 TPa for SWNTs. Using this benchmark for SWNTs, most of the tests obtain this modulus within each test's scatter band. Only the data from the Cooper and Young tests predict higher moduli[42]. Their tests differ from those of others since they use Raman spectroscopy on a nanotube composite material to back calculate a modulus. They comment that the results are for an idealized random three-dimensional fiber orientation that is not likely and would increase the modulus greatly.

It is notable that the experimental tests have not yet been able to determine any other material property of CNTs, such as the shear modulus or Poisson's ratio. Again, this lack of data is understandable, due to the current limits of testing at the nanoscale. This leaves the predictions of other elastic constants to atomistic simulations.

1.4 Molecular Simulations and Results

A set of published simulation results is tabulated in Table 1.B, that represents a good cross-section of published material property predictions. Results from both MM and QM simulations are listed.

In contrast with the experimental data, these predictions have little to no scatter. If the moduli are viewed instead as tube stiffness, which takes the tube area into account, they are found to converge more tightly around a single value (corresponding with the standard ~1 TPa modulus). The modulus trends cited were typically small in nature, with the modulus varying slightly. In particular, the radial trends were isolated to very small diameter tubes and helical trends limited to a few percent difference from the listed value.

Table 1.2. Material property predictions of CNTs from molecular simulations

investigation	year	Young's modulus (TPa)	thickness (Å)	ν	potential / method	modulus trend**
Robertson et al.[45]	'92	1.06	3.4		local density function and TB	$1/r^2$, helicity
Yakobson et al.[20]	'95	5.5	0.66		TB	
†	'96	1.07	3.4	0.19	TB	
Yakobson et al.[20]	'96	1.07	3.4		TB	
Cornwell et al.[46]	'97	1	3.4		TB	$1/r^2$
Halicioglu[47]	'97	0.5	6.8		TB	radial
Lu (mwnt)[48]	'97	1.11	3.4		universal force	# of walls
Lu (swnt)[48]	'97	0.97	3.4		universal force	
Hernandez et al.[11]	'98	1.24*	3.4		density funct. theory (QM)	
Yao[49]	'98	1	3.4		universal force tight binding	$1/r^2$
Ozaki et al.[50]	'00	0.98	3.4		O(N)	
Troya et al.[9]	'03	1.16	3.4		PM3 (QM)	
†	'03	1.40	3.4		MSINDO (QM)	
Van Lier et al.[51]	'00	1.09	3.4	0.11	Hartree-Fock (QM)	helicity (small)
Zhou et al.[52]	'00	5.1	0.71		electronic band theory	$1/r^2$
Zhou	'01	0.76	3.4	0.32	LDF (QM)	
Belytschko et al.[8]	'02	0.94	3.4	0.29	modified Morse	

* actually computed a surface based modulus of 0.42 TPa-nm

** most trends were small in nature

(QM) quantum mechanics method

† focus on nonlinear responses (buckling, fracture)

Of the publications listed above, special attention should be paid to work that studied more than the prediction of Young's modulus for CNTs. Both Yakobson et al.[20] and Cornwell and Willie[46] used the TB potential to study the buckling behavior of SWNTs. They found that MM can predict buckling modes such as shell-wall buckling and crimping. Based on these results, Yakobson et al.[20] hypothesized that a thinner continuum section (corresponding to the pi-bond thickness, 0.66 Å), combined with classical shell theory matches the MM results better than the standard, thick section (layer separation distance, 3.4 Å). Liew et al.[53] extended these buckling studies to investigate SWNT bundles consisting of three or seven bundle regular arrays[53]. Cao and Chen[54] studied the buckling effects due to pure bending and compared their results with FE predictions. It is interesting to note that much like the results shown later in this study[55], the FE models predicted buckling strains favorably but sometimes had difficulty in predicting the same mode shapes. Hernandez et al. performed simulations and predicted moduli on general $B_xC_yN_z$ type nanotubes[11]. Belytschko et al.[8] performed fracture simulations using the Tersoff-Brenner potential. Che et al. extended the TB potential to better model long range intermolecular forces[56]. As an application they simulated the failure of a (10,10) nanotube in tension. However, Troya[9] argues that QM models are needed to properly model CNT fracture as the TB potential inaccurately describes these events.

1.5 Motivation and Goals

As discussed in the earlier sections, two standard continuum models exist for nanotubes. Both models use molecular phenomena to define characteristic geometries. They also make simplifying assumptions that may or may not be appropriate. The resulting material models are simple and easy to use in 'back of the envelope' style calculations. The thick wall standard model can predict macro-material properties and can be easily extended to incorporate MWNTs. While this model may work well for global responses, such as predicting the deflection of a MWNT cantilevered beam, it cannot model the crimping behavior associated with high bending curvatures. The thin walled model better suited for local instability modeling, such as shell wall buckling[20]. However, it was not tested for MWNTs or SWNTs of large aspect ratios. A membrane model was

published that was verified for a large range of aspect ratios, walls and responses. However, it is a FE model that has a complex derivation that requires either coding or acquisition of the authors' code for implementation[25].

Therefore, a more comprehensive, yet simple, continuum material model for nanotubes is desired and is the goal of this work. It should be usable for the 'back of the envelope' calculations that are important for engineers when quick results are needed. It should also be robust enough to be employed in more sensitive analyses that may require more complex analyses. This model should be able to predict both local and global mechanical responses for various loads. For example, it should be able to predict crimping for long aspect ratio nanotubes in bending. It should also be applicable for SWNTs, MWNTs or as a base for composite material models. It was decided that the formulation of the model should also adhere to common engineering practices for obtaining material properties. Thus, the approach taken here will mirror what an engineer would face when given a cylinder of an unknown metal alloy. This material may be anisotropic, directionally dependent or nonlinear. Therefore, a number of tests will be employed to determine which assumptions are acceptable, and to develop the model. The material properties will then be calculated using continuum mechanics relationships. This engineering approach also dictates that continuum assumptions will not be made from molecular phenomenon. Instead, they will be calculated or based solely on test results. Because of the exhaustive and precise experimental testing required, molecular simulations will be employed rather than physical testing.

The development of this model is approached in three steps. First, a material model for a SWNT will be developed using MM simulations. The MM simulations will serve to mimic traditional material property tests. Simple tests, such as tension and torsion, will be used to build the continuum model. More complex tests, such as buckling, will be simulated to validate the model. Next, the model will be extended to MWNTs. Here the major test will be modeling the interwall interactions due to the van der Waal forces. The model should be robust enough to handle back of the envelope calculations or the complex responses requiring sensitive analysis of independent interwall movement. These models will also be developed and verified using MM simulations.

1.6 Methodology

The basic approach taken to develop and verify a comprehensive continuum model for nanotubes, and nanotube composites, is loosely a three step process and is listed below.

1. Perform virtual experiments (simulated mechanical experiments) using MM
 - create a nanotube model; relax its structure; apply loads and find minimum energy deformation state
 - data obtained are energy and atomic position results (deformed structure)
 - examples: tension and torsion tests
2. Develop a continuum model
 - check the deformed state of the structure to verify that continuum deformation laws are being obeyed by the MM model
 - choose a continuum model, by making basic assumptions, which may be fully defined by the tests performed. Develop analytical equations to describe loading responses in terms of deformation and energy and solve for the unknowns
 - examples: isotropic, linear, thin shell model (E,v,t)
3. Verify continuum model
 - perform new virtual experiments for loadings different from those used in part 2 and compare with continuum model predictions
 - examples: buckling and bending

The first step, virtual experiments, will be detailed in full in the next subsection. The second and third steps should be relatively straightforward for engineers and will not be detailed. An additional step, designated by the asterisk, may be added to prove the utility of the model by predicting the response of a potential engineering application.

1.6.1 *Virtual Experiments*

The simulated experiments are designed to mimic standard material properties tests. Traditional material property tests generally give the experimentalists overall load and some deformation data. Virtual experiments give the modeler gross or detailed energy data and full deformation data. Thus the major difference in data is the exchange of force for energy, combined with a detailed set of deformations. During model development, simple tests such as tension or torsion are preferred. For verification, more complex tests such as buckling, cantilever bending or four point bending are preferred.

The creation of a MM model of a nanotube reduces to estimating the initial positions of the atoms, choosing the atom type, and defining the bond connectivity. This is

analogous to placing the nodes, choosing the element type and defining the nodal connectivity in FE models. The next step however is very important to MM. In FE the strain energy of the initial or the reference configuration is assumed to be zero, while in MM this energy must be found. The estimated atomic positions are very unlikely to correspond to the minimum energy position of the structure(s). Thus, the energy of the input structure must be minimized before deformations are applied to the structure. In molecular mechanics, minimization occurs by allowing atoms to move freely until the system converges to a minimum energy structure. The global minimum energy structure is termed the relaxed structure, and this process is sometimes called relaxation. Failure to perform this step will invalidate all subsequent results. Often the input geometry will be very poor, with high bond strains or contain high contact regions (overly close non-bonded neighbors). Thus, the first minimization algorithm must be able to deal with poor structures. Steepest descent is one good choice for this step. These algorithms often have difficulties converging to tight tolerances; therefore, the first minimization is usually cut short so that a more powerful algorithm may be used. The Newton-Raphson method typically converges faster near energy wells and is often a good choice. Newton-Raphson requires the Hessian matrix (second derivatives) and may be unwieldy for very large structures. Nanotubes are very tight structures and it is relatively easy to find their global minimum.

Exceptions include stability events such as buckling which take more care. Thus a converged structure can be assumed to be the minimum energy structure.

Once a relaxed structure has been found, the virtual test may be performed. The load is applied by estimating a deformed structure. Like the input structure, this estimation will not be the minimum energy configuration, thus another minimization routine must be performed. To keep the desired deformation state, boundary conditions must be applied to the structure. Thus for a tension test, boundary conditions may be applied to the end atoms (simulating grips), allowing the inner atoms to move to minimum energy positions. Two types of boundary conditions are possible, a fixed atom position constraint or a force based position restraint. The fixed atom position boundary condition removes the chosen atoms from the minimization moving routines. This condition is analogous to a fixed nodal displacement of zero in all three direction in FE analysis. The second condition

imposes a force potential to keep the chosen atoms near their original positions. Thus, it is energetically less favorable to move atoms far from their starting point. This force constraint creates difficulties analyzing a test, however it can be useful during initial relaxation minimization.

The virtual tests are performed in discrete steps. An energy minimization is performed for each desired deformation step. The discrete set of data at each step creates a ramped, load history with energy as a function of deformation. Some tests, such as a tension test, are straightforward in execution. Others, such as a buckling test, may require more complicated procedures like perturbations to the estimated deformation to obtain converged results. Likewise, cantilever bending tests require convergence studies to properly apply the load. Whenever more complicated procedures are required, the procedure will be detailed in the relevant section.

Chapters two through five are written as papers for possible publication in refereed journals. Thus repetition of some of the material in them is unavoidable.

1.7 References

1. Iijima, S., *Helical microtubules of graphitic carbon*. Nature, 1991. **354**(7 Nov.): p. 56-58.
2. Jamieson, V., *Carbon nanotubes roll on*. Physics World, 2000. **13**(6).
3. Yu, M.-F., O. Lourie, M.J. Dyer, K. Moloni, T.F. Kelly and R.S. Ruoff, *Strength and breaking mechanism of multiwalled carbon nanotubes under tensile loads*. Science, 2000. **287**(Jan. 28): p. 637-640.
4. Barber, A.H., I. Kaplan-Ashiri, S.R. Cohen, R. Tenne and H.D. Wagner, *Stochastic strength of nanotubes: An appraisal of available data*. Composites Science and Technology, 2005. **65**(2380-2384).
5. Falvo, M.R., G.J. Clary, R.M. Taylor, V. Chi, F.P. Brooks, S. Washburn and R. Superfine, *Bending and buckling of carbon nanotubes under large strain*. Nature, 1997. **389**(6651): p. 582-584.
6. Zhao, Q., M.B. Nardelli and J. Bernholc, *Ultimate strength of carbon nanotubes: A theoretica study*. Physical Review B, 2002. **65**.
7. Stone, A.J. and D.J. Wales, *Theoretical studies of icosahedral C₆₀ and some related species*. Chemical Physics Letters, 1986. **128**(5-6): p. 501-503.
8. Belytschko, T., S.P. Xiao, G.C. Schatz and R.S. Ruoff, *Atomistic simulations of nanotube fracture*. Physical Review B, 2002. **66**(22).
9. Troya, D., S.L. Mielke and G.C. Schatz, *Carbon nanotube fracture - differences between quantum mechanical mechanisms and those of empirical potentials*. Chemical Physics Letters, 2003. **382**(1-2): p. 133-141.

10. White, C.T., D.H. Robertson and J.W. Mintmire, *Helical and rotational symmetries of nanoscale graphitic tubules*. Physical Review B, 1992. **47**(9): p. 5485-5488.
11. Hernandez, E., C. Goze, P. Bernier and A. Rubio, *Elastic Properties of C and BxCyNz Composite Nanotubes*. Physical Review Letters, 1998. **80**(20): p. 4502-4505.
12. Calvert, P., *A recipe for strength*. Nature, 1999. **399**(20 May): p. 210-211.
13. Thostenson, E.T., Z. Ren and T.-W. Chou, *Advances in the science and technology of carbon nanotubes and their composites: a review*. Composites Science and Technology, 2001. **61**: p. 1899-1912.
14. Baughman, R.H., A.A. Zakhidov and W.A.d. Heer, *Carbon Nanotubes- the Route Toward Application*. Science, 2002. **297**(August 2): p. 787-792.
15. Ajayan, P.M., L.S. Schadler, C. Giannaris and A. Rubio, *Single-Walled Carbon Nanotube-Polymer Composites: Strength and Weakness*. Advanced Materials, 2000. **12**(10): p. 750-753.
16. Jaffe, R., J. Han and A. Globus, *Formation of carbon nanotube based gears: quantum chemistry and molecular mechanics study of the electrophilic addition of o-benzene to fullerenes, graphene and nanotubes*. nanotechnology, 1997. **8**(3): p. 95-102.
17. Tuzun, R.E., D.W. Noid and B.G. Sumpter, *The dynamics of molecular bearings*. Nanotechnology, 1995. **6**: p. 64-74.
18. Yu, M.-F., B.I. Yakobson and R.S. Ruoff, *Controlled sliding of pullout of nested shells in individual multiwalled carbon nanotubes*. Journal of Physical Chemistry B., 2000. **104**: p. 8764-8767.
19. Gates, T.S., G.M. Odegard, S.J.V. Frankland and T.C. Clancy, *Computational materials: Multi-scale modeling and simulation of nanostructured materials*. Composites Science and Technology, 2005. **65**: p. 2416-2434.
20. Yakobson, B.I., C.J. Brabec and J. Bernholc, *Nanomechanics of carbon tubes: instabilities beyond linear response*. Physical Review Letters, 1996. **76**(14): p. 2511-2514.
21. Ru, C.Q., *Degraded axial buckling strain of multiwalled carbon nanotubes due to interlayer slips*. Journal of Applied Physics, 2001. **89**(6): p. 3426-3433.
22. Pantano, A., M.C. Boyce and D.M. Parks, *Nonlinear structural mechanics based modeling of carbon nanotube deformation*. Physical Review Letters, 2003. **91**(14).
23. Pantano, A., D.M. Parks and M.C. Boyce, *Mechanics of deformation of single- and multi-wall carbon nanotubes*. Journal of the Mechanics and Physics of Solids, 2004. **52**: p. 789-821.
24. Bower, C., R. Rosen, L. Jin, J. Han and O. Zhou, *Deformation of carbon nanotubes in nanotube-polymer composites*. Applied Physics Letters, 1999. **74**(22): p. 3317-3319.
25. Arroyo, M. and T. Belytschko, *Finite element methods for the non-linear mechanics of crystalline sheets and nanotubes*. International Journal for Numerical Methods in Engineering, 2003. **59**: p. 419-456.

26. Li, C. and T.-W. Chou, *Elastic moduli of multi-walled carbon nanotubes and the effect of van der Waals forces*. Composites Science & Technology, 2003. **63**: p. 1517-1524.
27. Kao, J., *A molecular orbital based molecular mechanics approach to study conjugated hydrocarbons*. Journal of the American Chemical Society, 1987. **109**(13): p. 3817-3835.
28. Leach, A.R., *Molecular Modeling, Principles and Applications 2nd ed.* 2001, Harlow, Eng.: Prentice Hall.
29. Allinger, N.L., Y.H. Yuh and J.-H. Lii, *Molecular Mechanics. The MM3 Force Field for Hydrocarbons*. Journal of the American Chemical Society, 1989. **111**(23): p. 8551-8566.
30. Ponder, J.W., *Tinker Molecular Modeling Package*. 2000, Washington University in St. Louis: St. Louis.
31. Brenner, D.W., *Empirical potential for hydrocarbons for use in simulating the chemical vapor deposition of diamond films*. Physical Review B, 1990. **42**(15): p. 9458-9471.
32. Brenner, D.W., O.A. Shenderova, J.A. Harrison, S.J. Stuart, B. Ni and S.B. Sinnott, *A second-generation reactive empirical bond order (REBO) potential energy expression for hydrocarbons*. Journal of Physics, 2002. **14**: p. 783-802.
33. Kollman, P.A., *Amber*. 1995.
34. Tuzun, R.E., D.W. Noid, B.G. Sumpter and R.C. Merkle, *Dynamics of fluid flow inside carbon nanotubes*. Nanotechnology, 1996. **7**: p. 241-246.
35. Wong, E.W., P.E. Sheehan and C.M. Lieber, *Nanobeam Mechanics: Elasticity, Strength and Toughness of Nanorods and Nanotubes*. Science, 1997. **277**(Sept. 26): p. 1971-1974.
36. Salvétat, J.-P., J.-M. Bonard, N.H. Thomson, A.J. Kulik, L. Forro, W. Benoit and L. Zuppiroli, *Mechanical properties of carbon nanotubes*. Applied Physics A, 1999. **69**: p. 255-260.
37. Tomblor, T.W., C. Zhou, L. Alexseyev, J. Kong, H. Dai, L. Liu, C.S. Jayanthi, M. Tang and S.-Y. Wu, *Reversible electromechanical characteristics of carbon nanotubes under local-probe manipulation*. Nature, 2000. **405**(15 June): p. 769-772.
38. Yu, M., B. Files, S. Arepalli and R. Ruoff, *Tensile loading of ropes of single wall carbon nanotubes and their mechanical properties*. Physical Review Letters, 2000. **84**(24): p. 5552-5555.
39. Treacy, M.M.J., T.W. Ebbesen and J.M. Gibson, *Exceptionally high Young's modulus observed for individual carbon nanotubes*. Nature, 1996. **381**(June 20): p. 678-680.
40. Qian, D., G.J. Wagner, W.K. Liu, M.-F. Yu and R.S. Ruoff, *Mechanics of carbon nanotubes*. Applied Mechanics Review, 2002. **55**(6): p. 495-533.
41. Krishnan, A., E. Dujardin, T.W. Ebbesen, P.N. Yianilos and M.M.J. Treacy, *Young's modulus of single-walled carbon nanotubes*. Physical Review B, 1998. **58**(20): p. 14013-14019.
42. Cooper, C.A. and R.J. Young, *Investigation into the deformation of carbon nanotubes and their composites through the use of Raman spectroscopy*. Proceedings of SPIE, 2000. **4098**: p. 172-181.

43. Lourie, O. and H. Wagner, *Evaluation of Young's modulus of carbon nanotubes by micro-raman spectroscopy*. Journal of Materials Research, 1998. **13**(9): p. 1471-1524.
44. Poncharal, P., Z.L. Wang, D. Ugarte and W.A.d. Heer, *Electrostatic deflections and electromechanical resonances of carbon nanotubes*. Science, 1999. **283**: p. 5407.
45. Robertson, D.H., D.W. Brenner and J.W. Mintmire, *Energetics of nanoscale graphitic tubules*. Physical Review B, 1992. **45**(21): p. 45-48.
46. Cornwell, C.F. and L.T. Wille, *Elastic properties of single-walled carbon nanotubes in compression*. Solid State Communications, 1997. **101**(8): p. 555-558.
47. Halicioglu, T., *Stress calculations for carbon nanotubes*. Thin Solid Films, 1998. **312**: p. 11-14.
48. Lu, J.P., *Elastic properities of carbon nanotubes and nanoropes*. Physical Review Letters, 1997. **79**(7): p. 1297-1300.
49. Yao, N. and V. Lordi, *Young's modulus of single-walled carbon nanotubes*. Journal of Applied Physics, 1998. **84**(4): p. 1939-1943.
50. Ozaki, T., Y. Iwasa and T. Mitani, *Stiffness of single-walled carbon nanotubes under large strain*. Physical Review Letters, 2000. **84**(8): p. 1712-1715.
51. Lier, G.V., C.V. Alsenoy, V.V. Doren and P. Geerlings, *Ab initio study of the elastic properties of single-walled carbon nanotubes and graphene*. Chemical Physics Letters, 2000. **326**: p. 181-185.
52. Zhou, X., J. Zhou and Z. Ou-Yang, *Strain energy and Young's modulus of single-wall carbon nanotubes calculated from electronic energy-band theory*. Physical Review B, 2000. **62**(20): p. 13692-13696.
53. Liew, K.M., C.H. Wong and M.J. Tan, *Tensile and compressive properties of carbon nanotube bundles*. Acta Materialia, 2006. **54**(225-231).
54. Cao, G. and X. Chen, *Buckling of single-walled carbon nanotubes upon bending: Molecular dynamics simulations and finite element method*. Physical Review B, 2006. **73**.
55. Sears, A., *Experimental validation of finite element techniques for buckling and postbuckling of composite sandwich shells*, in *Mechanical Engineering*. 1999, Montana State University, Bozeman: Bozeman.
56. Che, J., T. Cagin and W.A.G. III, *Studies of fullerenes and carbon nanotubes by an extended bond order*. Nanotechnology, 1999. **10**: p. 263-268.